On the Annual Rossby Wave in the Tropical North Pacific Ocean[1]

GARY MEYERS[2]

Department of Oceanography, University of Hawaii, Honolulu 96822

(Manuscript received 22 June 1978, in final form 29 January 1979)

ABSTRACT

Annual variation in the depth of the 14°C isotherm (i.e., the main thermocline) throughout the tropical Pacific Ocean between 30°N and 30°S is studied on the basis of 156 000 bathythermographs. Large-amplitude variations are confined in the region between 4 and 15°N. Near 6°N the variations in depth propagate westward. Near 12°N they have almost the same phase across the ocean from the American coast to 145°E. These variations are approximately consistent with a simple model that permits an oceanic response to local Ekman pumping, modified by nondispersive, baroclinic Rossby waves forced by the wind. Near 12°N, the rate of change in thermocline depth is nearly in phase with the Ekman pumping velocity, with only a minor but significant contribution coming from Rossby wave propagation. This type of response depends critically on variations in the eastern boundary region. Near 6°N, the westward propagating variations are generated by relatively large variability in Ekman pumping in the eastern Pacific, and apparently travel into the western Pacific as free nondispersive Rossby waves. Deficiencies of the model are also discussed.

1. Introduction

The variation in strength and thermal structure of the Pacific Equatorial Currents in response to annual forcing by the trade winds is an example of air-sea interaction on the largest possible scale. Large-scale interactions are currently being studied intensively in attempts to increase our understanding of climatic change. The purpose of this study is to describe the annual variation in thermal structure in the tropical Pacific Ocean and to test whether or not it is consistent with a simple, two-layered β-plane model. The model is driven by wind stress and the only permitted wavelike response is the nondispersive, baroclinic Rossby wave.

Two processes in the model cause vertical displacements of the thermocline. The first is the divergence in the Ekman layer, called Ekman pumping (Ekman, 1905; Greenspan and Howard, 1963). The second is the planetary, geostrophic divergence inherent on a rotating sphere, which has been clearly and heuristically explained by Stommel (1957).

Several studies carried out during the last decade have established the need for this investigation. Annual variation of the North Equatorial Current was first observed during the Trade Wind Zone Oceanography expedition in 1964 and 1965 (Seckel, 1968). Maximum strength of the current was found in the fall of 1964. A later study by Wyrtki (1974) of the dynamic topography of the sea surface based on all the available oceanographic station data and on sea level observed at islands revealed that the North Equatorial Current and the Countercurrent in the central Pacific are strongest from September to December and weakest from March to May. The South Equatorial Current in contrast is strongest from March to May. Annual variation in the North Equatorial Current was related to the trade winds by Meyers (1975), who found that vertical displacements of the thermocline in the central Pacific are nearly in phase with the Ekman pumping velocity calculated from the wind stress. White (1977) suggested that the agreement in phase occurs only near 150°W, but not at other longitudes, because in addition to local Ekman pumping, a forced Rossby wave propagates across the ocean from its source region at the eastern boundary. Data presented in this paper will show that the wave suggested by White (1977) is not the dominant annual signal in the North Equatorial Current, possibly due to the boundary condition used. More recently, DeWitt and Leetma (1978) analyzed data from the EASTROPAC expedition in 1967 and 1968 and found that cruise-to-cruise differences in thermocline depth are in phase with Ekman pumping at 119°W between 4 and 15°N.

While it has been established that annual variations in the equatorial currents occur, their general

[1] Hawaii Institute of Geophysics Contribution No. 946.

[2] Present affiliation: Scripps Institution of Oceanography, University of California, San Diego, La Jolla 92093.

0022-3670/79/040663-12$07.00

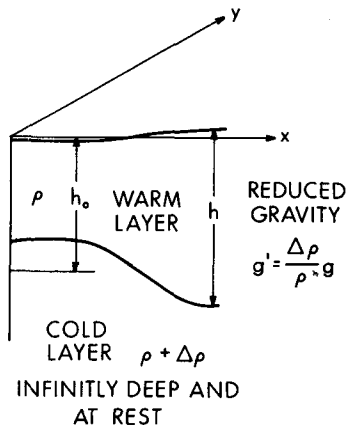

FIG. 1. Two-layered model. Symbols are defined in the text.

description throughout the tropical Pacific is still lacking. In this paper, the areas of largest variations are identified and described. Tests are made to determine whether or not these variations are consistent with the Ekman pumping/Rossby wave model.

2. Data sources and data processing

In order to study climatological aspects of the thermal structure with the largest possible data set, the mechanical bathythermograph (MBT) and expendable bathythermograph (XBT) data in the archives of the National Oceanographic Data Center were merged into a data set which contained approximately 156 000 observations. The method used to reduce these data to monthly isothermal depths on a 2° latitude by 10° longitude grid has been discussed in detail by Meyers (1978). The analysis was guided by several features of the variability in thermal structure noted by Wyrtki *et al.* (1977). Variation of temperature within the depth range of the thermocline is largely due to vertical displacements of the thermocline and not to changes in the intensity of the vertical temperature gradient. Consequently, variations in the depth of the thermocline are adequately represented by the depth of a single isotherm. The depth of the 14°C isotherm was chosen because it indicates strength of the North and South Equatorial Currents better than shallower isotherms. It is below the level of the maximum vertical density gradient, whose stability shields it from temperature fluctuations associated with heat exchange through the sea surface. Also, it is above the subsurface layer where the vertical temperature gradient is weak, making isotherm depth a poor indicator of vertical displacements.

Annual variation in the trade wind field over the Pacific Ocean was studied on the basis of 5 million wind observations made by ships. The data sources and data processing have been discussed in a technical report (Wyrtki and Meyers, 1975a,b). Wind stress was calculated from the ships' observations and reduced to monthly values on a 2° latitude by 10° longitude grid. The annual variation of the wind field has been discussed in detail in a separate article (Wyrtki and Meyers, 1976).

3. Theory of large-scale, low-frequency variations in tropical currents

a. The vorticity equation

The physical processes that govern the variability of large-scale, low-frequency tropical currents (excluding currents at the equator) are believed to be the divergence set up at the surface by the wind stress, called Ekman pumping, and the planetary geostrophic divergence inherent on a rotating sphere, called the β-effect (Yoshida, 1955; Veronis and Stommel, 1956; Stommel, 1957; Yoshida and Mao, 1957; Fedorov, 1961; Gill and Niiler, 1973; Meyers, 1975; McCreary, 1976, 1977; White, 1977, 1978; DeWitt and Leetma, 1978). The essential physics is contained in the vorticity equation for motion with very large space and time scales (McCreary, 1977, p. 22):

$$h_t - \frac{\beta g' h_0}{f^2} h_x = -\left(\frac{\tau^y}{f}\right)_x + \left(\frac{\tau^x}{f}\right)_y .$$

The model is a two-layered ocean which has a warm upper layer of thickness h and density ρ and an infinitely deep bottom layer of density $\rho + \Delta\rho$ (Fig. 1). The reduced gravity is g'. The coordinates x, y, t are distance eastward, distance northward and time, and the subscripts are partial derivatives. The Coriolis parameter is f and β is f_y. Annual variations in the zonal and meridional wind stress divided by density are τ^x and τ^y. The mean thickness of the upper layer is h_0. The only permitted wavelike response of this model is the nondispersive, baroclinic Rossby wave. Internal gravity waves, coastal and equatorial Kelvin waves, and dispersive Rossby waves are not permitted. The equation is valid in regions more than 5° from the equator when the space scale of the motion exceeds 500 km and the time scale exceeds three months (McCreary, 1977; Meyers, 1978).

The following transformations yield an equation which is convenient for discussion. Let

$$\left.\begin{aligned} h' &= h_0 - h, \quad x' = -x \\ W &= (\tau^y/f)_x - (\tau^x/f)_y \\ c &= \frac{\beta g' h_0}{f^2} \end{aligned}\right\} .$$

Then the equation becomes

$$h'_t + ch'_{x'} = W. \qquad (1)$$

The rate of change in depth of the thermocline is h', the Ekman pumping velocity is W, and the planetary geostrophic divergence inherent on a rotating sphere is $ch'_{x'}$. Note that derivatives with respect to y (latitude) do not appear in (1) which means that the latitudinal variability in W and c can be incorporated into analytic solutions (White, 1977). Also the x' coordinate can be replaced by the distance from the eastern boundary. These features of the model allow for a wide range of flexibility in testing the oceanic responses to meridionally and zonally varying wind fields.

A solution to the homogeneous form of (1) which is proportional to $\exp[i(\kappa x - \omega t)]$, where κ and ω are wavenumber and frequency yields the dispersion relationship for very long, nondispersive, baroclinic Rossby waves which travel westward with phase speed c (Veronis and Stommel, 1956, Fig. 1; Lighthill, 1969, Fig. 2).

b. Simple solutions

Two simple solutions to (1) have been discussed by White (1977, 1978). The simplest involves only the dynamics of the f-plane (i.e., β is set equal to zero). The thermocline in this case is moved vertically by local Ekman pumping. White (1977) also discussed the case of zonally uniform pumping across an ocean with an eastern boundary. The solution is a modulated, westward traveling wave with phase speed $2c$. Physically it is the superposition of the response to local Ekman pumping and a Rossby wave radiating from the eastern boundary. The Rossby wave is generated by an interaction between the local forcing and the condition that the eastern boundary be a streamline. The mathematical expression of this boundary condition, $h_b(t)$, is

$$h_b(t) = 0. \tag{2}$$

The modulated wave suggested by White (1977) is not the dominant signal in the tropical North Pacific, as shown in Section 3, possibly because the boundary condition (2) is not correct. The condition implicitly assumes that there is no longshore component to the wind. Nor does it allow for changes in thermocline depth at the equator, which are rapidly propagated poleward as Kelvin waves. It is known from observations that large, annual vertical displacements of the thermocline occur near the eastern boundary. These ageostrophic displacements can be taken into account without resorting to an ageostrophic model by solving (1) with the eastern "boundary" moved to a point seaward of the eastern boundary layer. The observed variation in h can be used as a boundary condition at this point.

Observations presented in the next section suggest that

$$h_b(t) = \int_0^t W dt \tag{3}$$

is the correct offshore boundary condition in some areas. Physically it represents local Ekman pumping.

Two more simple solutions are now discussed. In the case of zonally uniform forcing having the form

$$W = A \cos(\omega t), \tag{4}$$

while the solution with offshore boundary condition (3) is

$$h = \frac{A}{\omega} \sin(\omega t). \tag{5}$$

Physically this represents local Ekman pumping at all x.

In the case of zonal variation in forcing having the form of a standing wave, i.e.,

$$W = A \sin(\kappa x) \cos(\omega t), \tag{6}$$

the solution is

$$h = \frac{A}{2c\kappa''} \sin(\kappa'' x) \sin(\kappa' x - \omega t) + \frac{A}{2c\kappa'} \sin(\kappa' x) \sin(\kappa'' x - \omega t), \tag{7}$$

where

$$\kappa' = \tfrac{1}{2}(\kappa + \omega/c), \quad \kappa'' = \tfrac{1}{2}(\kappa - \omega/c).$$

Note that boundary conditions (2) and (3) are identical in this case. The solution for a wavenumber (κ) of the wind field nearly equal to the wavenumber of the free response ω/c is particularly interesting. The resonant solution in the limit as κ approaches ω/c is

$$h = \frac{A}{2\omega} [\kappa x \sin(\kappa x - \omega t) + \sin(\kappa x) \sin(\omega t)]. \tag{8}$$

This wave grows with distance from the eastern boundary but does not become exceedingly large unless $\kappa x \gg 1$. Its traveling component propagates westward at phase speed c.

The main points of the two simple solutions is that the Ekman pumping/nondispersive Rossby wave model permits a local oceanic response to the Ekman pumping as in (5) and a response that propagates westward at c and grows, as in (8).

c. General solution for arbitrary forcing

A general solution for arbitrary forcing is given below. Solutions for the observed wind field will be shown later and compared to observations. The time harmonic nature of annual forcing is not immediately exploited in order to show that the model can also be used in studies of the oceanic response to interannual variability in the wind field.

For an arbitrary forcing function $W(x,t)$, an arbitrary offshore boundary condition $h_b(t)$ and the initial condition $h_i(x,0) = 0$, the Laplace transform of the solution is

$$H(k,s) = \frac{w(k,s)}{(kc + s)} + \frac{cH(0,s)}{(kc + s)},$$

where k is the transform parameter for x, s the transform parameter for t, $w(k,s)$ the forcing function transformed in space and time, and $H(0,s)$ the boundary condition transformed in time. Inverse transformation in k and application of the convolution theorem yield

$$H(x,s) = \frac{1}{c}\int_0^x e^{-(s/c)(x-\zeta)}w(\zeta,s)d\zeta + H(0,s)e^{-(s/c)x}.$$

Inverse transformation in s and another application of the convolution theorem yield

$$h(x,t) = \frac{1}{c}\int_0^x \int_0^t \delta\left[t - \tau - \frac{(x-\zeta)}{c}\right]W(\zeta,\tau)d\tau d\zeta + \int_0^t \delta\left[t - \tau - \frac{x}{c}\right]h_b(\tau)d\tau,$$

where δ is the Dirac-delta function. The solution is independent of the initial condition after a time interval L/c, where L is the length of the zonal segment of ocean being studied. Using the inequalities $t - (x - \zeta)/c > 0$, $\zeta \geq 0$ and $\tau \leq t$, and properties of the Dirac-delta function, the integral over τ yields the solution

$$h(x,t) = \frac{1}{c}\int_0^x W\left[\zeta, t - \frac{(x-\zeta)}{c}\right]d\zeta + h_b\left(t - \frac{x}{c}\right). \quad (9)$$

Solutions for the observed annual variation in Ekman pumping velocity are easily calculated by letting W be a function of the form

$$W = A(x)\cos(\omega t) + B(x)\sin(\omega t), \quad (10)$$

where $A(x)$ and $B(x)$ are the annual harmonic Fourier coefficients of the observed Ekman pumping velocity. They are piecewise-continuous, linear functions between grid points.

4. Observed variations

Annual variations in the Ekman pumping velocity and in the depth of the 14°C isotherm are described in this section. The observations are used to test if they are consistent with the model developed in Section 3. The test suggests regions where the model and observations should be compared in greater detail.

The trade winds vary during the year with the strongest winds in the winter and spring hemisphere. The wind stress curl and Ekman pumping velocity, however, are relatively insensitive to the changes in wind strength, and depend mainly on the location of the Intertropical Convergence Zone (ITCZ) which changes latitude throughout the year (Wyrtki and Meyers, 1976). The extreme southward and northward positions are reached during the spring and the fall. Variation of wind stress curl in the eastern Pacific also depends on the formation of a monsoon wind blowing into Central America (Sadler, 1976) during the summer. Variation of wind stress curl in the southwestern Pacific occurs along the southern flank of a trough whose axis runs from the northern Coral Sea to and beyond Fiji during the southern summer.

The Ekman pumping velocity was computed on a 2° latitude by 10° longitude grid. The method used to evaluate the curl operator has been discussed in Wyrtki and Meyers (1975a). Values at the equator were calculated from a simple, frictional model developed by McKee and Gill (Gill, 1975). The equatorial calculation is discussed in detail in Meyers (1978). The annual (first harmonic) amplitude of the variation in Ekman pumping velocity is shown in Fig. 2. The month during which it is at a maximum value (upward) is also shown at a few key locations. The outstanding feature of this map is that pumping is largely confined to the equator and the eastern North Pacific. The largest extra equatorial values (15 m per month) are located at 6°N. The amplitude in the South Pacific exceeds 5 m per month only in a small area. The zonal variation in phase is shown in Fig. 3. In general, the phase is shown at latitudes which have a large amplitude. Maximum pumping in the region between 12 and 18°N occurs during August (240°) and September (270°) across the entire Pacific. The intense pumping near 6°N in the eastern Pacific is at a maximum in March (90°); however, the phase changes by more than six months in crossing the ocean at this latitude. The spatial structure of the Ekman pumping velocity in the tropical Pacific is by no means simple. Averaging it over longitude or latitude as other investigators have done can be misleading.

The observed variations in the depth of the 14°C isotherm will be discussed next. The tropical Pacific thermocline on average is characterized by a system of nearly zonally oriented ridges and troughs (Fig. 4) which separate the North Equatorial Current, the North Equatorial Countercurrent and the South Equatorial Current (Knauss, 1963). The Countercurrent ridge is located near 10°N between the North Equatorial Current and Countercurrent. The Countercurrent trough is located near 5°N between the Countercurrent and the South Equatorial

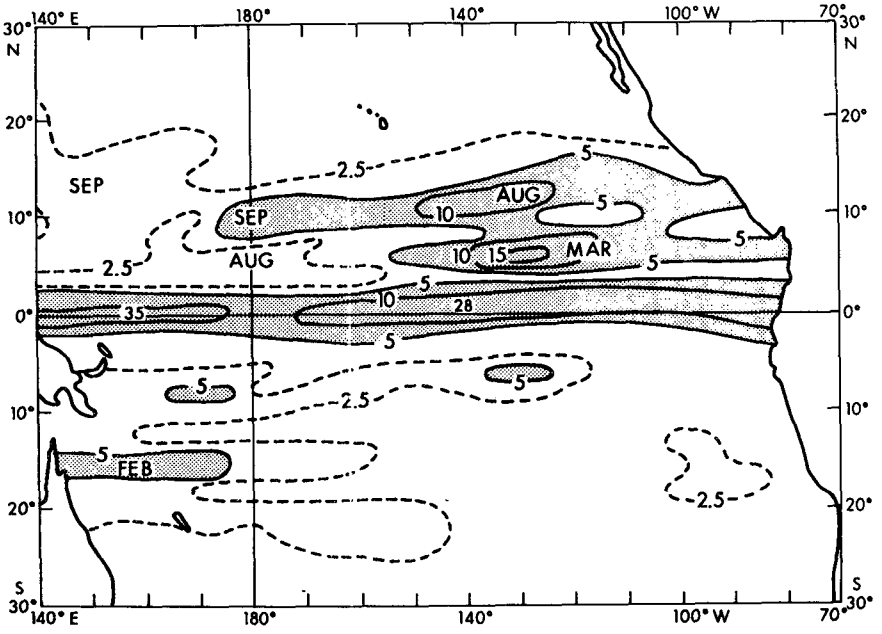

FIG. 2. Annual amplitude W of the Ekman pumping velocity (m per month). The region where W exceeds 5 m per month is shaded. The month of maximum upward values is indicated at a few locations.

Current. The near equatorial ridges at 2°N and 2°S divide the South Equatorial Current into branches which flow on either side of the equator.

The ridges and troughs change in depth throughout the year. The displacement of the depth of the 14°C isotherm (i.e., the main thermocline) from its mean position during November is shown in Fig. 5. This is a month of extreme development. Arrows on the contours indicate the direction of inferred changes in geostrophic flow. During November the Countercurrent ridge is high while the Countercurrent trough is low. Consequently, the North Equatorial Current and the Countercurrent are stronger than normal, especially in the central Pacific. The map also shows strengthening of the South Equatorial Current between about 4°N and 4°S and weakening between 4°S and 10°S.

The variations in the southeastern Pacific are based almost entirely on observations taken during the EASTROPAC expedition and did not appear in the earlier analysis of thermal structure by Wyrtki (1964). It is not yet clear whether the variations shown in this area are truly annual variations or cruise-to-cruise differences. Unfortunately, the study of annual variations in the South Pacific is limited by data sparseness. The westward increase in phase of the Ekman pumping velocity (Fig. 3) in the region from the equator to 16°S suggests the possibility for resonance. A more complete study of the South Pacific will be in order only when more observations have been accumulated.

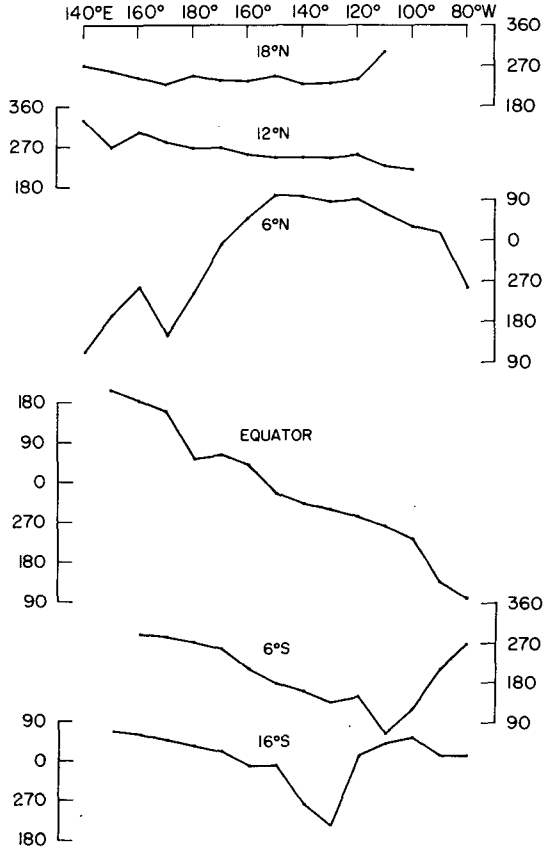

FIG. 3. Phase of the annual variations in Ekman pumping velocity.

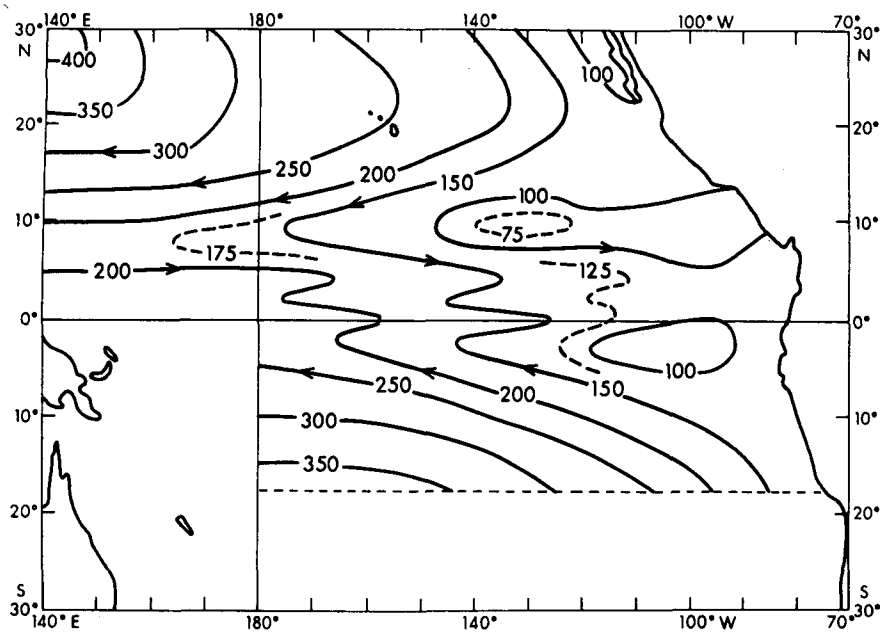

FIG. 4. Mean depth (m) of the 14°C isotherm.

The first harmonic amplitude of variation in the depth of the 14°C isotherm is shown in Fig. 6. The month of maximum displacement (upward) is shown at key locations. The outstanding feature of this map is that the large amplitudes are again largely confined to the Northern Hemisphere and the maximum amplitudes are aligned with maximum Ekman pumping at 6 and 12°N. The large variations in the thermocline extend westward to 140°E, in contrast to the intense Ekman pumping which is confined to the eastern Pacific. Apparently the β-effect allows propagation of energy into the western Pacific. The zonal variation in phase is shown in Fig. 7. The variations at 6°N increase in phase toward the west from the American coast to 145°E which is indicative of westward propagation.

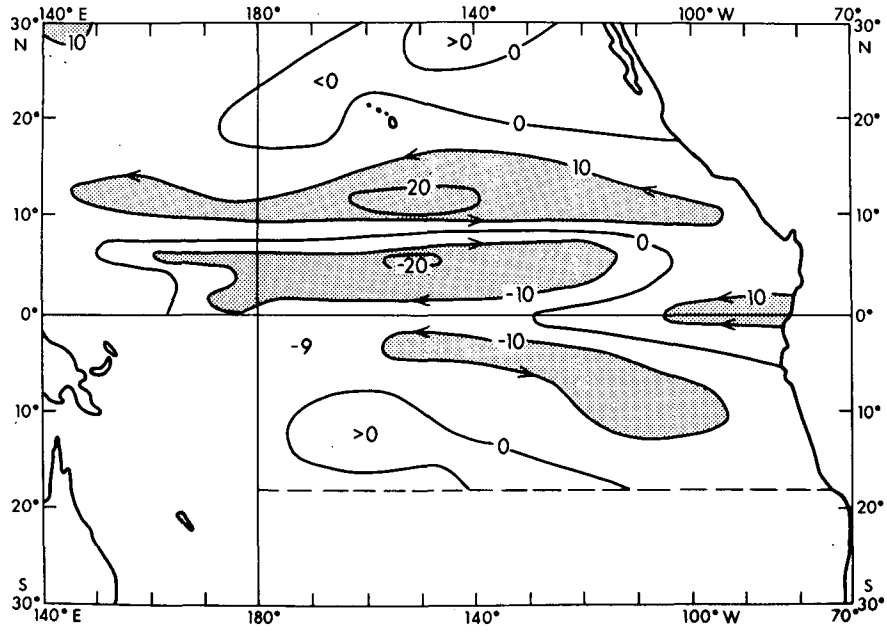

FIG. 5. Displacement (m) of the 14°C isotherm in November. The region where displacements exceed 10 m is shaded.

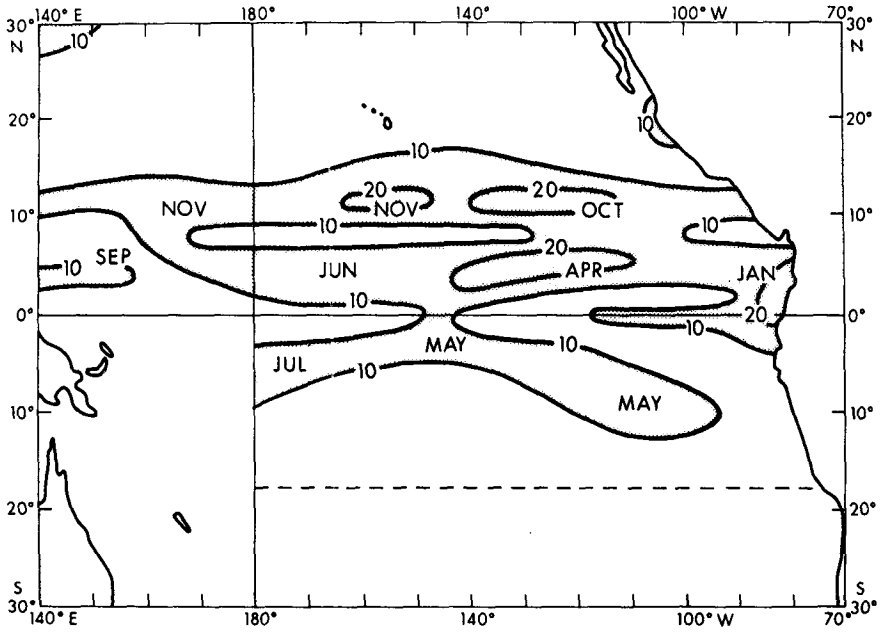

FIG. 6. Annual amplitude (m) of variations in the depth of the 14°C isotherm. The region where the amplitude exceeds 10 m is shaded. The month of maximum upward values is indicated at a few locations.

In contrast, the dominant variations at 12°N change only two months in phase between 105°W and 145°E. The spatial structure of phase at 12°N shows that the wave proposed by White (1977, Fig. 7) is not the dominant annual signal in the North Equatorial Current. Detection of this wave will require a more powerful statistical analysis than used in this study.

A test to find the regions where the observed variations are approximately consistent with the Ekman pumping/nondispersive Rossby wave model was made as follows. The test is designed to look for agreement in large-scale features of the spatial distribution of each term in (1), rather than numerical agreement at each grid point. Monthly displacements (h_E) were calculated from the Ekman pumping velocity (W) at each grid point by evaluating the integral

$$h_E(t) = \int_0^t W dt' - \langle h_E \rangle.$$

The angle braces indicate the annual mean value. Monthly displacements (h_G) caused by the geostrophic divergence were also calculated from the observed depth of 14°C by evaluating

$$h_G(t) = \int_0^t c h_x dt' - \langle h_G \rangle.$$

The nondispersive phase speed c was calculated assuming $g'h_0 = 5 \times 10^4$ cm^2 s^{-2} (White, 1977). The calculated displacements $h_E(t)$ and $h_E(t) + h_G(t)$

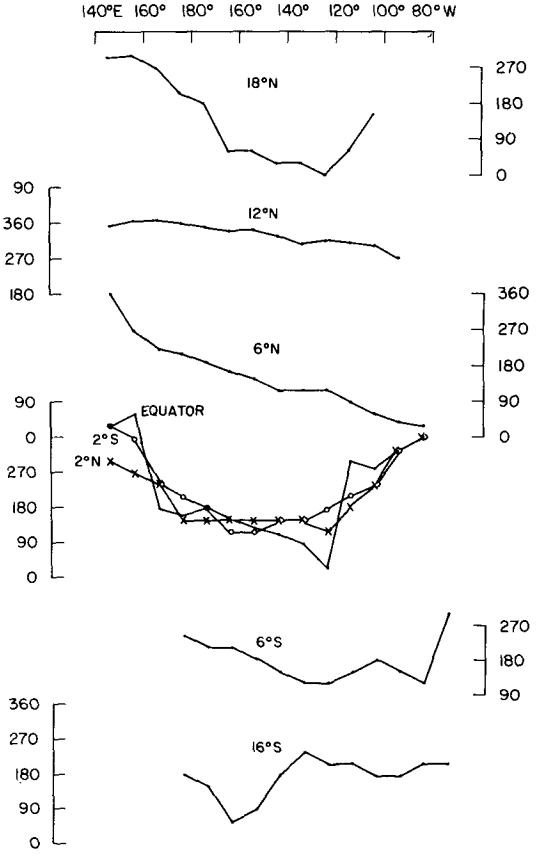

FIG. 7. Phase of annual variations in the depth of the 14°C isotherm.

were compared to the observed variations h at each grid point by calculating the correlation coefficient for the 12 monthly values.

Areas where the correlation coefficient between h_E and h exceeded 0.87 are shaded in Fig. 8. The correlation coefficient of two sinusoidal curves, $\cos\omega t$ and $\cos(\omega t + \phi)$, is $\cos\phi$, and equals 0.87 if the lag is one month. The figure indicates that the Ekman pumping velocity is in phase with the rate of change in depth of 14°C in the region between 10 and 15°N across the Pacific from the eastern boundary to 155°E. The amplitudes of these variations also agree quite well, as shown in Section 5. Two other large areas of phase agreement are found centered at 24°N, 155°E in the western Pacific and 10°S, 105°W in the eastern Pacific. Notably absent from the regions of phase agreement is the area between 4 and 8°N which has both large observed variations and Ekman pumping velocities. Addition of the geostrophic divergence yields calculated displacements $h_E + h_G$ which improve the map in this region (Fig. 9). The implication is that the phase of annual variations in strength of the North Equatorial Current and Countercurrent are consistent with a model that incorporates only Ekman pumping and geostrophic divergence. Note that the regions of agreement are the regions where the amplitude of the depth of the 14°C isotherm is large (Fig. 6). Failure to find agreement in the regions where the amplitude is small may indicate that the signal was not extracted from the noise by the statistical procedures used.

5. Variations at 6°N and 12°N

The variations at 6 and 12°N are now compared in detail to the Ekman pumping/nondispersive Rossby wave model. The solution (9) discussed in Section 3 is used to calculate the oceanic response to the observed Ekman pumping. The observed variation in the depth of the 14°C isotherm ~500 km from the Central American coast was used for the offshore boundary condition. The results suggest that the main features of the observed variability across the ocean can be calculated from the wind stress. However, perhaps more important, the comparison reveals deficiencies of the model that will have to be improved in future attempts to develop a viable model of the tropical Pacific Ocean.

Solutions to (9) for the observed wind field were calculated as follows. The Ekman pumping velocity calculated from the wind stress was represented by an equation of the form (10). The first harmonic coefficients A and B were calculated at grid points by standard harmonic analysis. The amplitude and phase of the Ekman pumping have already been discussed (Figs. 2 and 3). The functions $A(x)$ and $B(x)$ were assumed to be piecewise-continuous, linear functions between grid points.

The phase speed c of the nondispersive Rossby wave must be known before the solution (9) can be evaluated. Two approaches were used to determine c. The first approach (method I) was to find the value of c that gives the best agreement in phase. This was accomplished by calculating the correlation coefficient between observed variations and

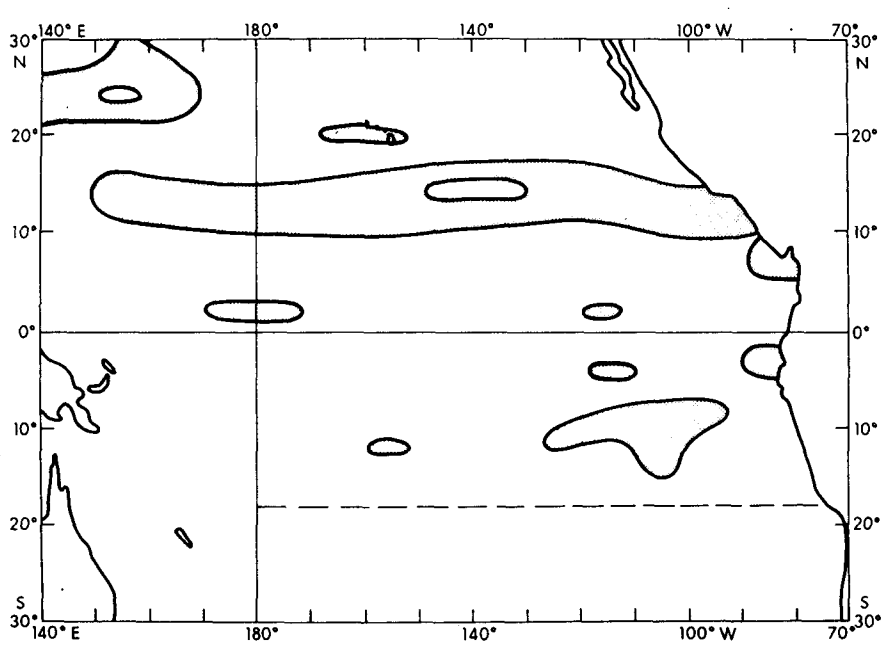

FIG. 8. Region (shaded) where the rate of change in the depth of the 14°C isotherm is in phase with the Ekman pumping velocity, determined by a method explained in the text.

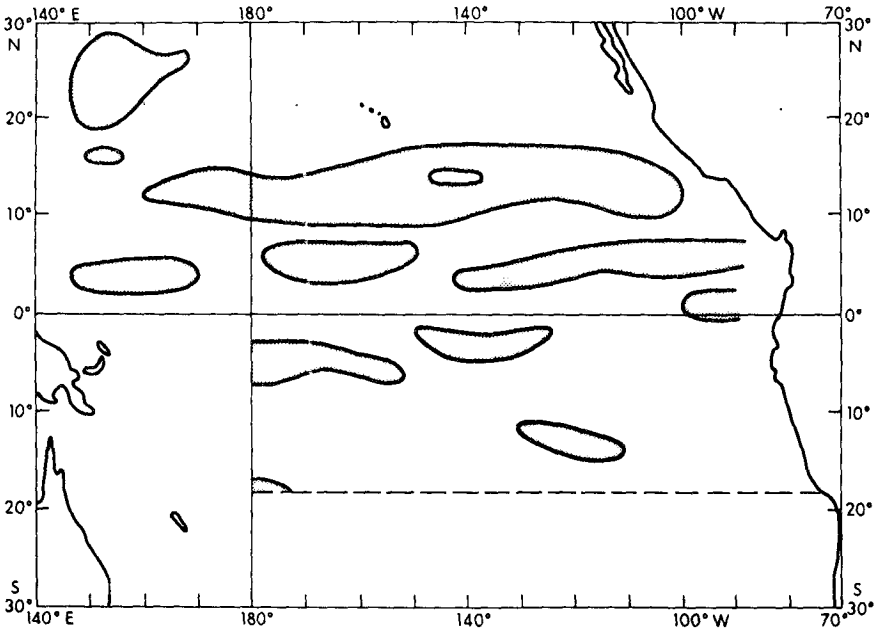

FIG. 9. Region (shaded) where the rate of change in the depth of the 14°C isotherm is in phase with the sum of geostrophic divergence and Ekman pumping velocity, determined by a method explained in the text.

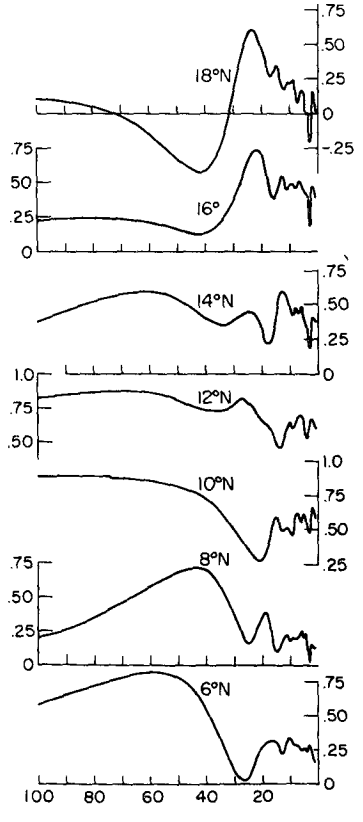

FIG. 10. Correlation coefficient between observed variations and variations calculated from the wind stress using Eq. (9) as a function of the nondispersive Rossby wave phase speed c (cm s^{-1}).

the solution for values of c varying from 1 to 100 cm s^{-1}. The correlation coefficients are shown for latitudes between 6 and 18°N in Fig. 10. Maximum correlation coefficients emerge distinctly at 6, 8, 16 and 18°N. Relative maximum correlation coefficients within the range of reasonable values (5–60 cm s^{-1}) occur for 12 and 14°N. The best values of c as a function of latitude are shown in Fig. 11. Clearly, c does not follow a $1/f^2$ dependence (shown by the dashed line), which will be discussed later. The best value of c at 10°N does not appear distinctly in Fig. 10. The plotted value in Fig. 11 was selected because it is at the end of a rapid rise in correlation.

The second approach for evaluating c (method II) was to determine it by measuring $g'h_0$ from the ob-

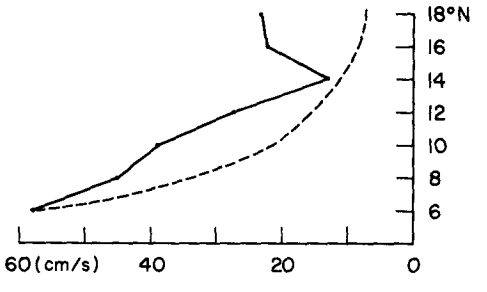

FIG. 11. The nondispersive Rossby wave phase speed c (cm s^{-1}) as a function of latitude. Plotted values give maximum correlation between observed variations and variations calculated from the wind stress using Eq. (9). The dashed line indicates $1/f^2$ dependence.

TABLE 1. First baroclinic equivalent depth $H^{(1)}$.

Latitude (°N)	Longitude (°W)	$H^{(1)}$ (cm)	Data source	Expedition
6	160	83	Reid (1965)	EQUAPAC
10	160	53		
18	160	90		
7	129	53	Reid *et al.* (1965)	Downwind
11	128	51		
19	125	57		

served density structure. This was done by evaluating the first baroclinic equivalent depth ($H^{(1)}$), then

$$g'h_0 = gH^{(1)}.$$

A method for evaluating $H^{(1)}$ in a multilayered ocean is given by Lighthill (1969, p. 86). This method was used for several oceanographic stations taken from standard sources (Reid, 1965; Reid *et al.*, 1965). Each standard depth was assumed to be the center of a layer of uniform density. Values of $H^{(1)}$, given in Table 1, were interpolated to 6 and 12°N and averaged between 160 and 128°W in order to evaluate c at each latitude. The result shows c equal to 65 cm s^{-1} at 6°N and 16 cm s^{-1} at 12°N. Note that the values of c determined by method II at 6°N is nearly the same as the value determined by Method I. The value at 12°N is smaller.

Observed and calculated variations at 6 and 12°N are shown in Figs. 12 and 13. Panel A shows observed variations. Panel B shows displacements calculated from only the Ekman pumping velocity neglecting the β-effect (called h_E in Section 4). Panel C shows the solution by method I, which has the highest possible correlation between the model and the observations. Panel D shows the solution by method II, with c determined by strict application of theory (Lighthill, 1969).

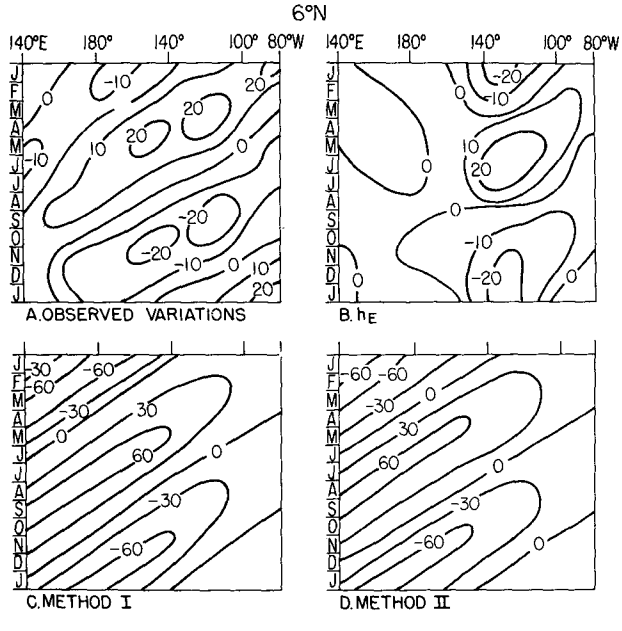

FIG. 12. (A) Observed variations (m) in the depth of 14°C at 6°N. (B) Displacements (h_E) caused by only Ekman pumping. (C) Displacements calculated from the wind stress with (9) by method I (explained in text). (D) Displacements calculated from the wind stress with (9) by method II (explained in text).

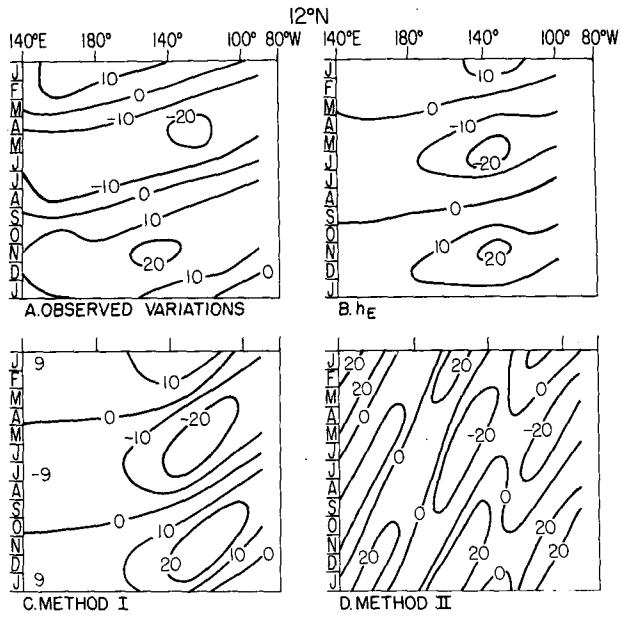

FIG. 13. As in Fig. 12 except for variations at 12°N.

The variations at 6°N (Fig. 12) are discussed first. The Ekman pumping displacements (panel B) are large only in the eastern Pacific. Clearly, Ekman pumping alone cannot account for the observed variations whose amplitude exceeds 10 m across the entire ocean. The Rossby wave phase speed c determined by method I (58 cm s^{-1}) and method II (65 cm s^{-1}) is essentially the same, giving the same solutions in panels C and D. Both show a wave generated in the eastern Pacific by the strong forcing. It grows rapidly from the coast to 140°W and propagates at the nondispersive speed c into the western Pacific, where the forcing is weak. The response calculated from the wind stress is similar in phase to the observed variations (panel A). The amplitude is too large in the central and western Pacific, possibly because the model does not allow dissipation or dispersive transport of energy.

It is instructive to compare the variations at 6°N to the simple models discussed in Section 3. The observed pumping at 6°N can be schematically represented by (6) if we let κ be $2\pi/L$, where $L/2$ is the distance from 80 to 160°W (Fig. 2), and W be zero outside the region $0 \leq x \leq L/2$. Thus, the forcing occurs over half a wavelength. The solution is (7) in the forced region $0 \leq x \leq L/2$, and it radiates

from $x = L/2$ nondispersively into the free region $x > L/2$. Note that ω/κ in this case equals 56 cm s^{-1}, which nearly equals the value of c determined by both method I and method II. Therefore, the nearly resonant solution (8) is appropriate. This solution correctly gives a wave which grows toward the west in the forced region and propagates westward at phase speed c. The phase lag ϕ between h and W at the position of maximum forcing $\kappa x = \pi/2$ is

$$\phi = \tan^{-1} \frac{2}{\pi} = 32°. \tag{11}$$

Thus the forced wave lags the maximum Ekman pumping velocity by approximately one month. The maximum observed Ekman pumping is located at 130°W (Fig. 2) and the observed phase lag there is nearly one month (Figs. 3 and 7) in agreement with the model.

The Ekman pumping/Rossby wave model produces the main features of the observed variations at 6°N, aside from the incorrect amplitude calculated for the central and western Pacific. In particular, the intense pumping in the eastern Pacific can account for the large variations in the main thermocline observed in both the eastern and western Pacific at this latitude.

The variations at 12°N are discussed next (Fig. 13). The observed variations are largely consistent with displacements due only to local Ekman pumping (panels A and B), except in the western Pacific where observed variations are larger. The β-plane model gives better agreement in amplitude in the western Pacific (panel C), by allowing energy to propagate westward. However, only the solution by method I has the observed structure of variations in longitude and time. The solution by method II produces westward propagating features that are not observed in the ocean. The phase speed c in method I (27 cm s^{-1}) was chosen to optimize agreement with observations. It is larger than c determined by strict application of Lighthill's (1969) theory. No explanation of this discrepancy is known by the author. Unfortunately, this test of the Ekman pumping/Rossby wave model does not permit an unequivocal conclusion at 12°N. Either the β-effect is negligible and the observed variations are nearly due to Ekman pumping alone (panel B) or the nondispersive phase speed c is truly larger than expected (panel C).

It should be noted that the solution by method I (panel C) is critically dependent on the offshore eastern boundary condition. If it is changed to (2), the model again produces westward propagating features which are not observed in the ocean. The variations at 12°N apparently are similar to the simple solution (5) discussed in Section 2. An investigation into why boundary condition (3) seems to be the correct one at 12°N should be made in the future.

6. Summary and conclusions

Annual variation in the depth of the 14°C isotherm throughout the tropical Pacific Ocean has been described. The largest variations are found near 6 and 12°N. Near 6°N the variations propagate westward at nearly the phase speed of free non-dispersive Rossby waves. Near 12°N the zonal change in phase is only two months. A simple model which permits an oceanic response to Ekman pumping in the form of nondispersive Rossby waves is qualitatively consistent with the observed variations, but deficiencies of the model have been noted. The model produces variations which are too large at 6°N. Also it requires a larger than expected value of the nondispersive Rossby wave phase speed in order to correctly produce the observed variations at 12°N. One might be tempted to conclude that the model fails to simulate the annual cycle in thermocline depth in the tropical Pacific, as White (1978) concluded for the North Pacific. However, the model is not performing equally poorly at the lower latitudes. Some important features of the observed variations are produced by the model, as seen in Figs. 12 and 13, suggesting that at least part of the dominant physics of the annual waves is included in the model. Before the negative conclusion can be made, one might rather investigate whether or not the larger than expected phase speed is consistent with a more complete dynamical model, possibly allowing for an interaction between the annual waves and mean shear flow.

Acknowledgments. I am grateful to Professor Klaus Wyrtki for many helpful suggestions while serving as chairman of my Ph.D. dissertation committee. Julian McCreary clarified some ideas on resonance. Shikiko Nakahara and Bernie Kilonsky gave expert assistance in computer programming. This research was supported by the National Science Foundation as part of the North Pacific Experiment of the International Decade of Ocean Exploration; this support is gratefully acknowledged.

REFERENCES

DeWitt, P. W., and A. Leetma, 1978: A simple Ekman-type model for predicting thermocline displacement in the tropical Pacific. *J. Phys. Oceanogr.*, **8**, 811–817.

Ekman, W. W., 1905: On the influence of the earth's rotation on ocean-currents. *Ark. Mat. Astron. Fys.*, **2**, No. 11, 1–52.

Fedorov, K. N., 1961: Seasonal variations of equatorial currents in the ocean. *Problems in Dynamical Oceanography*, A. I. Fel'zenbaum, Ed., 156–160, [Trans. by I. Shlectman, Israel Program for Scientific Translations, 1968.]

Gill, A. E., 1975: Models of equatorial currents. *Proc. Symp. Numerical Models of Ocean Circulation*, Durham, NH, 1972, U.S. Nat. Acad. Sci., 181–203.

——, and P. P. Niiler, 1973: The theory of the seasonal variability in the ocean. *Deep-Sea Res.*, **20**, 141–177.

Greenspan, H. P., and L. N. Howard, 1963: On a time-dependent motion of a rotating fluid. *J. Fluid Mech.*, **17**, 384–404.

Knauss, J. A., 1963: Equatorial current systems. *The Sea*, Vol. 2, M. N. Hill, Ed., Interscience, 235–252.

Lighthill, M. H., 1969: Dynamic response of the Indian Ocean to onset of the southwest monsoon. *Phil. Trans. Roy. Soc. London*, **A265**, 45–92.

McCreary, J. P., 1976: Eastern tropical ocean response to changing wind systems: with application to El Niño. *J. Phys. Oceanogr.*, **6**, 623–645.

——, 1977: Eastern ocean response to changing wind systems, Ph.D. dissertation, University of California, San Diego, 156 pp.

Meyers, G., 1975: Seasonal variation in transport of the Pacific North Equatorial Current relative to the wind field. *J. Phys. Oceanogr.*, **5**, 442–449.

——, 1978: Annual variation in the depth of 14°C in the tropical Pacific Ocean, Ph.D. dissertation, University of Hawaii, Honolulu, 79 pp.

Reid, J. L., 1965: Intermediate waters of the Pacific Ocean. *Johns Hopkins Oceanogr. Stud.*, No. 2, 85 pp.

——, R. S. Arthur and E. B. Bennet, Eds., 1965: *Oceanic Observations of the Pacific: 1957*, Berkeley and Los Angeles, University of California Press, 705 pp.

Sadler, J. C., 1976: Comments on "Low-level flow over the GATE area during summer 1972". *Mon. Wea. Rev.*, **104**, 650–652.

Seckel, G. R., 1968: A time-sequence of oceanographic investigation in the North Pacific trade wind zone. *Trans. Amer. Geophys. Union*, **49**, 377–387.

Stommel, H., 1957: A survey of ocean current theory. *Deep-Sea Res.*, **4**, 149–184.

Veronis, G., and H. Stommel, 1956: The action of variable wind stresses on a stratified ocean. *J. Mar. Res.*, **15**, 43–75.

White, W. B., 1977: Annual forcing of baroclinic Rossby waves in the tropical North Pacific Ocean. *J. Phys. Oceanogr.*, **7**, 50–61.

——, 1978: The wind-driven seasonal cycle of the main thermocline in the mid-latitude North Pacific. *J. Phys. Oceanogr.*, **8**, 818–824.

——, 1964: The thermal structure of the eastern Pacific Ocean. *Deut. Hydrogr. Z. Erg.*, No. 6, 1–84.

——, 1974: Sea level and the seasonal fluctuations of the equatorial currents in the western Pacific Ocean. *J. Phys. Oceanogr.*, **4**, 91–103.

——, and G. Meyers, 1975a: The trade wind field over the Pacific Ocean. Part I. The mean field and the mean annual variation. Hawaii Inst. Geophys., Rep. No. HIG-75-1, 26 pp., 25 figs.

——, and ——, 1975b: The trade wind field over the Pacific Ocean. Part II. Bimonthly fields of wind stress 1950–1972. Hawaii Inst. Geophys., Rep. No. HIG-75-2, 16 pp., 138 figs.

——, and ——, 1976: The trade wind field over the Pacific Ocean. *J. Appl. Meteor.*, **15**, 698–704.

——, ——, D. McLain and W. Patzert, 1977: Variability of the thermal structure in the central equatorial Pacific Ocean. Hawaii Inst. Geophys., Rep. No. HIG-77-1, 32 pp., 16 figs.

Yoshida, K., 1955: An example of variations in oceanic circulation in response to the variations in the wind fields. *J. Oceanogr. Soc. Japan*, **11**, 103–108.

——, and H. L. Mao, 1957: A theory of upwelling of large horizontal extent. *J. Mar. Res.*, **16**, 40–57.